







SYMPOSIUM

Air Breathing and Suction Feeding Kinematics in the West African Lungfish, *Protopterus annectens*

Elska B. Kaczmarek ^{*,1}, Samantha M. Gartner [†], Mark W. Westneat [†] and Elizabeth L. Brainerd ^{*}

^{*}Department of Ecology, Evolution, and Organismal Biology, Brown University, Providence, RI 02912, USA; [†]Department of Organismal Biology and Anatomy, University of Chicago, Chicago, IL 60637, USA

From the symposium “Lesser known transitions: organismal form and function across abiotic gradients” presented at the annual meeting of the Society for Integrative and Comparative Biology, January 3–7 2022, in Phoenix, AZ, USA.

¹E-mail: elska_kaczmarek@brown.edu

Synopsis Research on the water-to-land transition tends to focus on the locomotor changes necessary for terrestriality. However, the evolution from water breathing to air breathing was also a necessary precursor to the invasion of land. Air is approximately 1000 times less dense and 50 times less viscous, and contains hundreds of times more oxygen than water. However, unlike the transition to terrestrial locomotion, breathing air does not require body weight support, so the evolution of air breathing may have necessitated smaller changes to morphology and function. We used X-ray reconstruction of moving morphology to compare the cranial kinematics of aquatic buccal pumping, such as that seen in suction feeding, with the aerial buccal pumping required for lung ventilation in the West African lungfish (*Protopterus annectens*). During buccal pumping behaviors, the cranial bones and associated soft tissues act as valves and pumps, and the sequence of their motions controls the pattern of fluid flow. Both behaviors are characterized by an anterior-to-posterior wave of expansion and an anterior-to-posterior wave of compression. We found that the pectoral girdle and cranial rib rotate consistently during air breathing and suction feeding, and that the muscle between them shortens during buccal expansion. Overall, we conclude that the major cranial bones maintain the same basic functions (i.e., acting as valves or pumps, or transmitting power) across aquatic and aerial buccal pumping. The cranial morphology that enables aquatic buccal pumping is well suited to perform air breathing and accommodates the physical differences between air and water.

Introduction

When an animal is able to perform two similar behaviors that interact with physically distinct abiotic media (such as water, air, sand, or solid ground), we expect that the animal must move very differently in each behavior and/or have specialized anatomy and physiology that allows them to be successful in each medium. The fish-to-tetrapod transition is an excellent example of this. During this major transformation, fish and tetrapodomorphs had to navigate the interface between air and water, which have vastly different physical properties. The fish-to-tetrapod transition encompassed adaptations to nearly all parts of fish anatomy, physiology, and behavior, including changes to the skin, eyes, ears, kidneys, reproductive structures

and behaviors, bones, fins, and olfaction, as well as to feeding, swallowing, breathing, and locomotor behaviors (Farmer 1999; Long and Gordon 2004; Sayer 2005; Coates et al. 2008; Clack 2009; Damsgaard et al. 2020; MacIver and Finlay 2021). In particular, the evolution of terrestrial locomotion matches our expectation that substantial changes are required to successfully adapt to a new physical medium. Terrestrial locomotion required the evolution of new morphology (weight-bearing limbs) and a new locomotor mode (limb-driven propulsion that resists gravity), both of which were distinct from those of their fish ancestors (Shubin et al. 2006; Coates et al. 2008).

Breathing air was also a necessary precursor to terrestriality and required interacting with a new physical

Advance Access publication July 7, 2022

Published by Oxford University Press on behalf of the Society for Integrative and Comparative Biology 2022. This work is written by (a) US Government employee(s) and is in the public domain in the US.

medium, but it may not match the expectation that it required large changes to morphology or kinematics. Air breathing evolved ~430 million years ago, in the shared ancestor of Sarcopterygii and Actinopterygii, which was about 50 million years before tetrapodomorphs moved onto land (Clack 2009; Betancur-R et al. 2017). Like terrestrial locomotion, the evolution of air breathing required new morphology (lungs) and a new behavior (surfacing, expiring air, and inspiring air; Brainerd 1994; Graham 1997). However, the physical challenges associated with air breathing are different from the requirements for terrestrial locomotion. Because most fish breathe air while staying mostly submerged, breathing air does not require the fish to support its body weight against gravity. However, pumping air into the lungs is a new biomechanical challenge. Fish solved this problem with a buccal pump: expanding and compressing the oropharyngeal cavity to draw air in and pump it back to inflate the lungs (Bishop and Foxon 1968). Fish had previously evolved buccal pumping as a solution to the problems of ventilating their gills and capturing food in water (Hughes 1965; Wainwright et al. 2015). In suction feeding, buccal expansion must be fast and forceful to suck in water and prey. In contrast, in air breathing, buccal compression must generate force to pump air into the lungs and inflate them, while countering the hydrostatic pressure of the surrounding water that is pushing in on the body wall (Brainerd and Ferry-Graham 2006). Although these behaviors are all forms of buccal pumping, they have different functional demands and interact with different media. We sought to investigate whether air breathing (aerial buccal pumping) requires specialized anatomy or behavior in comparison to suction feeding (an aquatic buccal pumping behavior).

Lungfish are well suited for addressing questions about the origin of air breathing. Lungfish are more closely related to tetrapods than to ray-finned fish (Rosen et al. 1981; Takezaki et al. 2004), and lepidosirenid lungfish are obligate air breathers, obtaining most of their oxygen from the air while also periodically ventilating their gills (Babiker 1979; Graham 1997). Because of their phylogenetic position and life history traits, lungfish are often looked to for insights into the fish-to-tetrapod transition, especially the transition to terrestrial locomotion (Aiello et al. 2014; Horner and Jayne 2014; King and Hale 2014; Granatosky et al. 2020).

Aside from locomotion, research on lungfish has examined their suction feeding and air breathing behaviors (Bishop and Foxon 1968; McMahon 1969; Bemis and Lauder 1986). These studies primarily documented anatomy, muscle activity via electromyography (EMG), kinematics of the lower jaw and hyoid, and pressure recordings (during air breathing). Regarding skeletal

kinematics, they found that, during both suction feeding and air breathing, buccal expansion was produced via lower jaw opening and neurocranial elevation, followed by ceratohyal depression. While these studies established a strong foundation for understanding the muscle activity and biomechanics of these behaviors, they were limited by the technology available at the time and in which bone motions they studied, thus limiting the capacity for comparing air breathing and suction feeding. Recent work by Gartner et al. (2022) examines lungfish suction feeding kinematics using X-ray reconstruction of moving morphology (XROMM), providing precise, 3D kinematic data for the cranium, lower jaw, and ceratohyals. However, the clavicles, cranial ribs, and associated musculature may also play important roles during these behaviors, and their motions have received much less attention. While it is known that the clavicles move during air breathing (Bishop and Foxon 1968), we do not know the magnitude of their motion, nor whether they move during suction feeding. Even less is known about the role of the cranial rib, a modified rib only found in lungfish that articulates with the occipital region of the cranium and is the attachment site for many muscles (Fig. 1). None of the prior studies of suction feeding and air breathing have drawn conclusions about the function of the cranial rib (Bishop and Foxon 1968; McMahon 1969; Bemis and Lauder 1986; Gartner et al. 2022).

Quantifying the kinematics of the cranial rib is important for addressing whether air breathing requires specialization in comparison to suction feeding. One possibility is that the cranial rib moves during air breathing but does not move during suction feeding, suggesting that the cranial rib functions in a specialized way during air breathing. It is also possible that the cranial rib does not move during air breathing but moves during suction feeding, also suggesting that its role is modified in air breathing. Lastly, it is possible that the cranial rib moves similarly in both behaviors, or does not move in either behavior, which would suggest that air breathing does not require specialized anatomy or behavior of the cranial rib in comparison to suction feeding. Similar predictions can be made for the other cranial bones, where different kinematics during air breathing would also suggest that air breathing requires specialized movement compared to suction feeding.

To test whether lungfish are using specialized anatomy, such as the cranial rib, or specialized behavior to breathe air, we compared the kinematics of air breathing to that of suction feeding. We recorded biplanar X-ray videos of air breaths, as well as a small number of suction strikes, in *P. annectens*. We then used the XROMM workflow to create precise and accurate 3D skeletal animations of those behaviors (Brainerd et al.

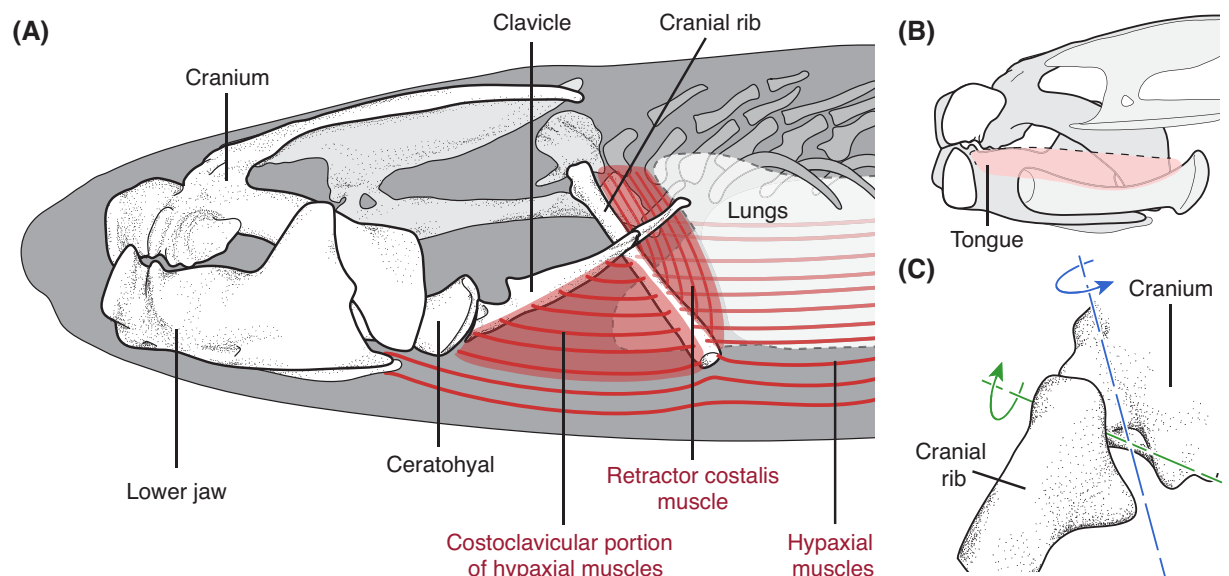


Fig. 1 Cranial musculoskeletal anatomy of West African lungfish, *Protopterus annectens*. **(A)** Lateral view of the animated bones (labeled), the hypaxial muscles, the costoclavicular portion of the hypaxial muscles (CCH), and the retractor costalis muscle. Note that, for clarity, not all bones of the head are shown. **(B)** Midsagittal cross section of the head, showing the position of the (fleshy, non-muscular) tongue just dorsal to the ceratohyal bone. **(C)** Posterolateral view of the costo-cranial joint, which connects the cranial rib and the exoccipital bone of the cranium. The axes of motion, estimated based on saddle-joint morphology, are shown in blue (primary axis) and green (secondary axis).

2010), which we used to measure skeletal kinematics and length changes of the costoclavicular portion of the hypaxial muscles. These data allowed us to (1) quantitatively describe the kinematics of air breathing, (2) determine the roles of the clavicles and cranial ribs during air breathing and suction feeding, and (3) compare the kinematics of these behaviors.

Materials and methods

Three West African lungfish (*P. annectens*) were acquired from the aquarium industry: Pa01 (standard length 48 cm, body mass 402 g), Pa02 (54 cm, 820 g), and Pa04 (54 cm, 710 g). *Protopterus annectens* were fed earthworms, protein pellets, and, occasionally, feeder fish. All husbandry and experimental procedures were approved by the University of Chicago Institutional Animal Care and Use Committee (Protocol 72,365). Data were collected from these individuals for Gartner et al. (2022), where Pa01, Pa02, and Pa04 are referred to as lungfish A, C, and B, respectively, and then additional data were collected for this study. After data collection, we observed in the CT scans that Pa02 had a dislocated jaw. Therefore, the data for the injured fish were not analyzed for this study.

Marker implantation

Each fish was anesthetized with a buffered MS-222 solution and implanted with radio-opaque markers in the bones and muscles (Supplementary Fig. S1).

Implantation techniques were consistent with those previously reported (Camp and Brainerd 2014), and are described here in brief. Radio-opaque markers (0.8 mm or 1.0 mm diameter tantalum spheres) were implanted into the following bones: seven in the cranium (specifically the pterygoid and supraorbital bones), three in the lower jaw, three to four in left clavicle, three in the left ceratohyal, and three in the right ceratohyal (Fig. 1, Supplementary Fig. S1). Three markers were also implanted in the right clavicle of Pa04. An electric drill (Dremel, Racine, WA, USA) was used to create press-fit holes in the upper jaw (pterygoid) and lower jaw because of the very high density of these bones. In all individuals, a hypodermic needle was used to implant three markers in the tongue and one marker next to the cranial rib, approximately 1.0 mm away from the bone (Supplementary Fig. S1). The tongue is a fleshy (not muscular) structure that is dorsal to the ceratohyals and cannot be moved independently of the ceratohyals (Fig. 1B). The motion of the tongue very closely matched the motion of the ceratohyals (Supplementary Fig. S2), so ceratohyal rotation was used as a proxy for tongue position.

Data recording

Biplanar X-ray video data of air breathing and suction feeding were recorded at 150 frames s^{-1} using Xcitex XC-2M high-speed video cameras (Xcitex, Woburn, MA, USA) in the University of Chicago XROMM facility. Two X-ray machines were used to capture two oblique lateral views, positioned at approximately a

right angle to each other, at 75–80 kV and 40 mA. The fish were transferred to a narrow tank for data collection (58.5 cm L × 9.2 cm W × 29.5 cm H) and then returned to their home tanks (35–55 gallons) after at most one hour. Images of standard grids and calibration objects were used to remove distortion introduced by the X-ray machines and calibrate the 3D space captured by both videos (Brainerd et al. 2010). Six breaths and one suction feeding strike were recorded from Pa01 and five breaths and three suction feeding strikes were recorded from Pa04. The videos of air breathing were subsampled to 75 frames s⁻¹ before analysis, while the videos of suction feeding remained at 150 frames s⁻¹. Air breathing is a much slower behavior than feeding, so subsampling the videos reduced the work required to track them without compromising data quality.

Computed tomography (CT) scans were taken of each individual using a Vimago L CT Scanner (Epica, Duncan, SC, USA). Polygonal meshes of the radio-opaque beads and of each implanted bone were segmented using Horos (v.3.3.6, Horos Project, horosproject.org) and edited in Geomagic 2014 (Research Triangle Park, NC, USA). Polygonal meshes of the markers were imported into Autodesk Maya 2018 (San Rafael, CA, USA), and their respective 3D coordinates were determined using custom scripts from the “XROMM Maya Tools” package (available at <https://bitbucket.org/xromm/xmalab>). Raw data for this study are publicly available and stored on the University of Chicago XMA Portal (<https://xromm.rcc.uchicago.edu/>). Video data are stored with their essential metadata in accordance with best practices for video data management in organismal biology (Brainerd et al. 2017).

XROMM animation

Skeletal kinematics were reconstructed using marker-based XROMM. XMALab 1.5.5 (Knörlein et al. 2016; software and instructions available at <https://bitbucket.org/xromm/xmalab>), which was used to undistort and calibrate the X-ray videos and to track the markers. Mean marker tracking precision in this study, measured as the mean of the standard deviation of the unfiltered inter-marker distances of the intraosseous markers, was 0.12 mm, and the maximum precision error was 0.27 mm across all trials. The 3D motion of each bone was then reconstructed using the “matools” R package, following the XROMM workflow described in Olsen et al. (2019) (available under matools R package at <https://github.com/aaronolsen>). Briefly, for bones that contained three or more markers, rigid body transformations were produced by smoothing the 3D marker coordinates and combining them with their respective

CT coordinates (using the “unifyMotion” function from “matools”). These rigid body transformations were applied to the skeletal bone meshes in Maya (2020, Autodesk), producing a 3D XROMM animation of each trial (Fig. 2). For bones with a linear set of markers (the left ceratohyal and the left clavicle of Pa04), virtual constraints were applied using the “matools” R package in accordance with anatomical constraints (e.g., cartilaginous symphysis between the left and right bones). For the cranial rib, two virtual points were placed on the cranium at the costo-cranial joint, dorsal and ventral to each other. These virtual points and the radio-opaque marker that was implanted next to the cranial rib were used to produce rigid body transformations using the “matools” R package.

Skeletal kinematics

The 3D XROMM animations were used to measure the motions of the lower jaw, ceratohyals, clavicles, and left cranial rib relative to the cranium. 3D rotations of the bones were measured using joint coordinate systems (JCSs), where an anatomical coordinate system (ACS) is attached to one bone, and a second ACS is attached to the cranium (Supplementary Figs. S3 and S4). For the lower jaw, both ACSs were aligned with the *z*-axis oriented mediolaterally, the *y*-axis oriented dorsoventrally, and the *x*-axis oriented rostrocaudally. For the ceratohyals and clavicles, the *z*-axis of the proximal ACS was aligned to the mediolateral axis of the head, and the *x*-axis of the distal ACS was aligned along the long axis of the bone. For the cranial rib, the *z*-axis of the proximal ACS was aligned to the primary axis of motion (“bucket-handle” motion, Brainerd et al. 2016; Capano et al. 2019) based on the morphology of the joint, and the *x*-axis of the distal ACS was aligned to the long axis of the bone. Each JCS measured translation and Euler angle rotations about the *x*-, *y*-, *z*-axis, following the right-hand rule and *zyx* order of rotation. Positive *z*-axis rotation indicated protraction and elevation. Negative *z*-axis rotation indicated retraction and depression. *Z*-axis rotations were standardized to start at 0° by subtracting their value at the start of each breath or strike, where the start of the behavior was defined as the start of lower jaw depression.

Timing of lung deflation and inflation

The start and end times for lung deflation and lung inflation were estimated based on close visual examination of the X-ray videos from each breath (gray shaded regions in Fig. 3B and C and Fig. 4B and C). These estimated time points were conservative, including slight changes in the brightness of the lungs in the X-rays. For one trial, the diameter of the

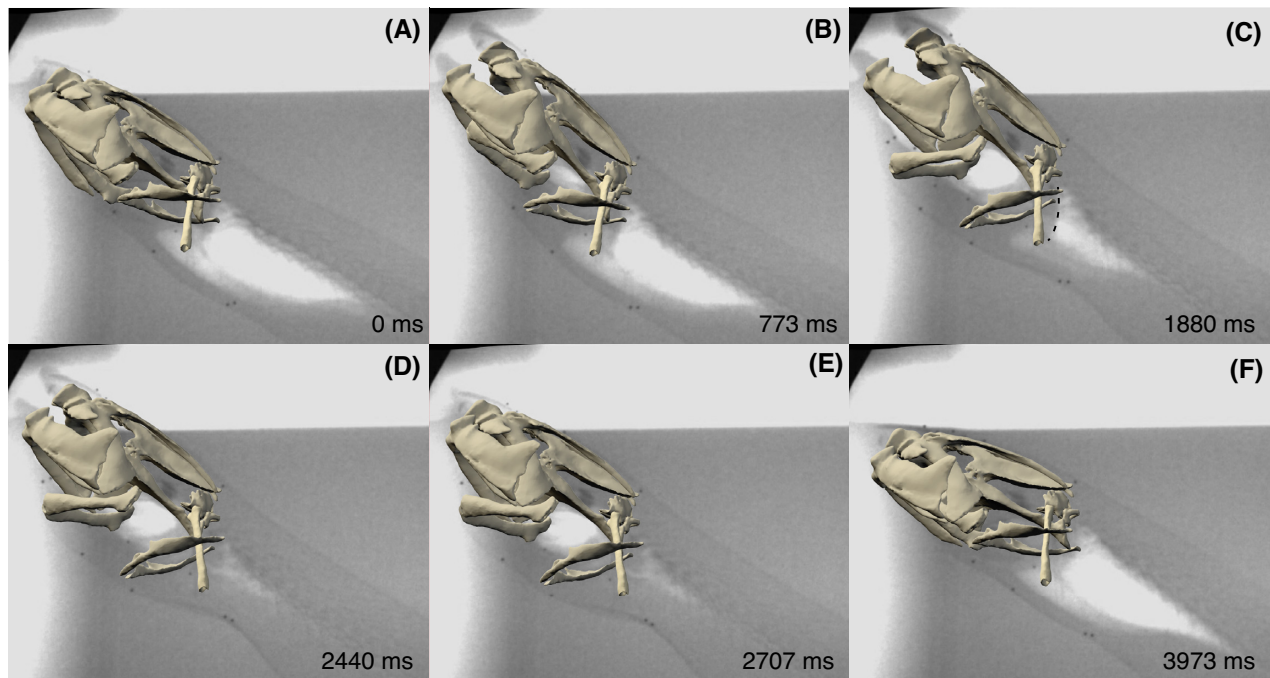


Fig. 2 A series of frames from an X-ray video and XROMM animation of a lungfish breathing air. **(A)** Start of the breath, defined as the start of lower jaw depression. **(B)** Start of lung deflation. **(C)** Peak ceratohyal depression. The dashed line indicates the shadow of the retractor costalis, which can also be seen in the other frames. **(D)** End of lung deflation. **(E)** Start of lung inflation. **(F)** End of lung inflation. See Fig. 1 for identification of the skeletal elements.

lungs was measured from a lateral X-ray video using XMALab (Fig. 3C), providing a proxy for lung volume. These data corresponded well to the visually estimated timing of lung deflation and inflation and also indicated that the estimated time points were conservative.

Normalizing time to breath duration

For the air breathing trials, time was normalized to the duration of the breath before the trials were averaged. The start of the breath was defined as the start of lower jaw depression. Although the cranial rib and clavicle are the last bones to finish protracting at the end of the breath, there was rarely a clear, consistent signal in their kinematics that could be used to define the end of the breath. Instead, elevation of the lower jaw, which had a clear signal at jaw closure, was used. The duration of the breath was defined as 125% (for Pa01) or 150% (for Pa04) of the duration from the start of jaw opening to the end of jaw closure. In other words, in all Pa01 breaths, the lower jaw closed at 80.00% breath duration, and in Pa04 breaths, the lower jaw closed at 66.66% breath duration. These percentages were chosen to best match the approximate end of clavicle protraction.

Muscle anatomy

The anatomy of the muscles that attach to the cranial rib was documented based on dissection of museum specimens and μ CT scans of Pa01 and Pa04 after staining with phosphomolybdic acid (PMA). Three specimens of *Protopterus aethiopicus* were obtained from the Harvard Museum of Comparative Zoology with permission to dissect (lot number MCZ: Ich:54,055). All three specimens were appropriately 20 cm long. The cranial muscles, including those attaching to the cranial rib, were dissected and photographed.

After data collection was completed for this study, Pa01 and Pa04 were euthanized, PMA stained, and μ CT scanned using a Phoenix V|tome|x CT scanner (Waygate Technologies, a Baker Hughes Company, Houston, TX, USA). The scans were visualized with Amira (Thermo Fisher Scientific, Waltham, MA, USA) to examine the anatomy of the muscles attaching to the cranial rib.

Muscle length changes

Changes in length of the costoclavicular portion of the hypaxial muscles (CCH, see below) were measured as the distance between two virtual landmarks that were placed on the left clavicle and left cranial rib in Maya (Supplementary Fig. S1). The positions of the landmarks were chosen based on the position and

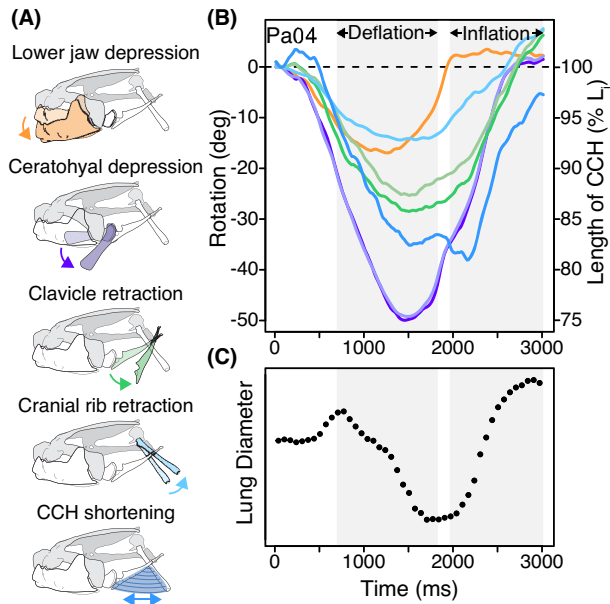


Fig. 3 Skeletal kinematics and lung diameter from a representative air breath. **(A)** Motion about the z-axis of the JCSs of the animated bones (see Supplementary Figs. S3 and S4 for JCS orientations), and shortening of the CCH muscle. Arrows indicate depression/retraction (negative rotation about the z-axes) and muscle shortening. **(B)** Z-axis rotations of animated bones and length change of the CCH during a representative air breath from Pa04. All curves were zeroed to their values at the start of the air breath. Negative values indicate depression/retraction and muscle shortening. Colors correspond to the bones shown in Fig. 3A. Note that for the ceratohyal and cleithrum, the lighter line represents the left bone and the darker line represents the right bone. **(C)** Dorsoventral diameter of the lungs was measured from the lateral X-ray video (e.g., Fig. 2) for the representative breath shown in **(B)**. Lung diameter serves as a proxy for lung volume. **(B** and **C)** Gray-shaded regions indicate the periods of lung deflation (first region) and inflation (second region).

orientation of fibers of the CCH. The distance between the muscle landmarks was calculated in R for each trial.

Results

Our central finding is that air breathing and suction feeding in *P. annectens* proceed along similar behavioral and kinematic sequences, with some important differences in duration (breathing occurs over a three-fold longer time period than feeding). The primary results of this study are anatomical information focused on the respiratory and feeding systems, including a previously undescribed cranial rib muscle, and comparisons of breathing and feeding mechanics.

Musculoskeletal anatomy of the cranial rib

Rib bones are connected by hypaxial muscles, and so, being a rib bone, the cranial rib is embedded in hypaxial muscles. Part of the hypaxial musculature passes su-

perficial to the cranial rib and clavicles and inserts on the ceratohyals anteriorly (Supplementary Fig. S5; along the way, it becomes the rectus cervicis muscle, which connects the clavicles to the ceratohyals, but the division between these muscles is not consistently described in prior literature; McMahon 1969; Bemis and Lauder 1986). Some of the deeper layers of hypaxial fibers are interrupted, and the fibers insert along the lateral and ventral surfaces of the clavicles and along the lateral surfaces and ventral ends of the cranial ribs.

An additional set of fibers originates on the cranial surface of the cranial ribs and inserts on the caudal surface of the clavicles (Fig. 1A). This region of muscle has been called the “anterior muscle of the cranial ribs” (McMahon 1969). In an effort to use more specific terminology, we refer to it as the costoclavicular portion of the hypaxial muscles (CCH). Shortening of this muscle would cause the clavicle and cranial rib to move closer together. The effect that has on skeletal motion depends on the concurrent activity of the other muscles that attach to these bones. Laterally, the superficial layers of these fibers appear continuous with the fibers of the hypaxials and rectus cervicis.

Caudal to the cranial rib is a retractor muscle, which has not been previously described (Figs. 1A and 2C). This muscle originates on the caudalmost end of the parasphenoid bone of the cranium and on the notochord in the region of the first two vertebrae. It inserts on the posterior surface of the cranial rib. Based on the position of this muscle and its fibers, we expect that shortening of this muscle would rotate the cranial rib posteriorly and dorsally, so we give it the latin name *M. retractor costalis*. Prior studies have measured EMG activity of the “posterior muscle of the cranial rib” (McMahon 1969) and the “rectus cervicis posterior” (Bemis and Lauder 1986), both of which refer to the hypaxial region that is just caudal to the cranial rib but is superficial to and separate from the retractor costalis.

The costo-cranial joint (between the cranial rib and the exoccipital bone of the cranium) has well-defined joint surfaces that suggest mobility of the cranial rib (Fig. 1C). The morphology of the joint appears to permit motion with two degrees of freedom, wherein the primary axis of rotation would best be described as retraction and protraction of the rib, and the secondary axis of rotation would best be described as adduction and abduction of the rib.

Air breathing behavior

Based on our X-ray videos and XROMM animations, we observed the following sequence of events during air breathing in our study individuals. First, the fish raised

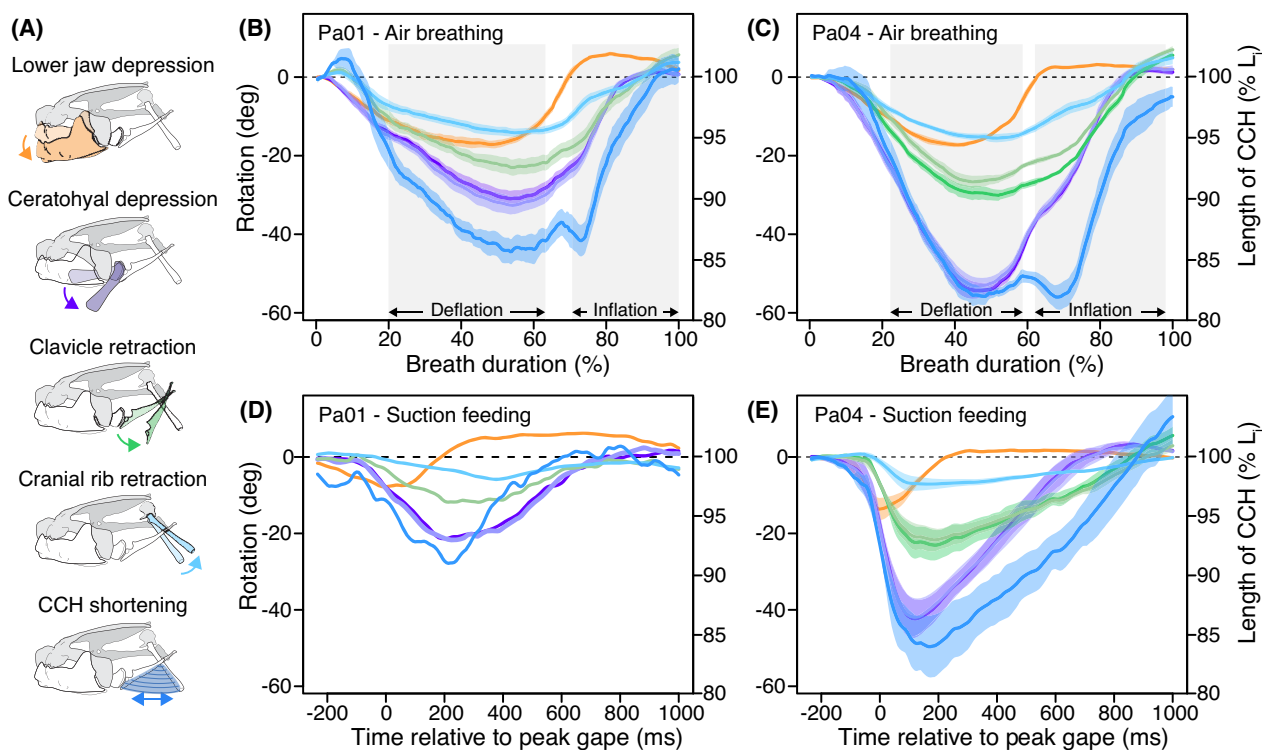


Fig. 4 Mean skeletal kinematics and muscle shortening during air breathing and suction feeding in Pa01 and Pa04. **(A)** Rotation about the z-axis of the JCSs of the animated bones (see Supplementary Figs. S3 and S4 for JCS orientations), and shortening of the CCH muscle. Arrows indicate depression/retraction (negative rotation about the z-axes) and muscle shortening. **(B and C)** Mean \pm s.e.m. z-axis rotations of the animated bones (left y-axis), and mean \pm s.e.m. length changes of the CCH (right y-axis) during air breathing in Pa01 ($n = 6$) and Pa04 ($n = 5$), respectively. Gray-shaded regions indicate the periods of lung deflation (first region) and inflation (second region). **(D and E)** Mean \pm s.e.m. z-axis rotations of the animated bones (left y-axis), and mean \pm s.e.m. length changes of the CCH (right y-axis) during suction feeding in Pa01 ($n = 1$) and Pa04 ($n = 3$), respectively. **(B, C, D, and E)** All curves were zeroed to their values at the start of the behavior. Negative values indicate depression/retraction and muscle shortening. Colors correspond to the bones shown in Fig. 4A. Note that for the ceratohyal and cleithrum, the lighter line represents the left bone and the darker line represents the right bone.

its head to the surface, typically compressing its buccal cavity as it rose, presumably to expel any water that remained. Only the tips of its jaws were raised above the surface (Fig. 2A). The expansion phase began as the fish depressed its lower jaw and started expanding its buccal cavity, allowing air to enter. Once air reached the back of the buccal cavity, lung deflation (i.e., expiration) started (Fig. 2B). The fish continued to expand the buccal cavity as the lungs emptied (Fig. 2C). The lungs are thought to deflate passively as a result of hydrostatic pressure pushing in on the compliant ventral body wall and the elasticity of lung tissue, but there may be some contribution from the smooth muscle that surrounds the lungs (Bishop and Foxon 1968; McMahon 1969). As soon as the expansion peaked, compression began, and lung deflation finished slightly after, as the jaws were closing. The lungs deflated almost completely, and the ventral body wall became concave (in a lateral view) in the region ventral to the median sac of the lungs (Fig. 2D). Once the lower jaw was closed, continued compression of the buccal cavity forced the air to inflate the lungs. During the start of lung inflation (i.e.,

inspiration; Fig. 2E), the tongue was not yet touching the roof of the mouth because the tongue and the ceratohyals (the tongue cannot be moved independently of the ceratohyals; Supplementary Fig. S5; Bemis and Lauder 1986; Gartner et al. 2022) were still elevating from their depressed position. Midway through lung inflation, the ceratohyals were fully elevated and the tongue was pressed against the cranium (Fig. 4B and C). Then the fish began to sink below the surface of the water as it finished compressing the buccal cavity and completed lung inflation (Fig. 2F). Nearly all of the air in the buccal cavity was forced into the lungs. Within a second or so of the end of compression, the fish typically slightly expanded the buccal cavity and compressed it again to flush a few small air bubbles out of the opercular openings.

In this study, aquatic gill ventilation was infrequent, so it was unclear whether the timing of the air breaths maintained the aquatic ventilatory rhythm. That is, it was unclear whether periodic gill ventilation continued up to the start of the air breath, the air breath took the place of a gill ventilation cycle, and then gill venti-

Table 1 Mean duration and magnitude and timing of bone rotation and muscle shortening during air breathing.

Variable		Pa01 (n = 6)	Pa04 (n = 5)	Combined
Breath duration (ms)		4533 ± 357	3213 ± 302	3933 ± 308
Lower jaw	Peak depression* (°)	−17.8 ± 1.21	−17.5 ± 0.6	−17.6 ± 0.7
	Time to peak depression (ms)	2147 ± 245	1272 ± 135	1749 ± 197
Ceratohyal (left)	Peak depression* (°)	−32.9 ± 2.33	−53.3 ± 2.0	−42.2 ± 3.5
	Time to peak depression (ms)	2451 ± 202	1501 ± 128	2019 ± 191
Clavicle (left)	Peak retraction* (°)	−23.3 ± 2.03	−27.0 ± 1.5	−25.0 ± 1.4
	Time to peak retraction (ms)	2498 ± 208	1467 ± 136	2029 ± 204
Cranial rib (left)	Peak retraction* (°)	−14.4 ± 1.01	−15.8 ± 1.0	−15.0 ± 0.7
	Time to peak retraction (ms)	2551 ± 227	1525 ± 204	2085 ± 218
Costoclavicular portion of hypaxial muscles (CCH, left)	Peak strain** (% L_i)	14.7 ± 1.08	18.5 ± 0.7	16.4 ± 0.9
	Time to peak shortening (ms)	2407 ± 195	1560 ± 132	2022 ± 177

*Negative values indicate depression or retraction.

**Positive values indicate muscle shortening. Mean ± s.e.m. are shown for each variable. Magnitude and timing of peaks were measured relative to start of behavior (start of lower jaw depression).

lation resumed immediately afterward, as observed by McMahon (1969).

Skeletal kinematics during air breathing

The time course of air breathing behavior was of long duration, typically occurring over 3–5 s, with some individual variability. When time was normalized to the duration of the breath (% breath duration), the sequence and timings of peak bone rotations were remarkably consistent within each individual and between the individuals (Fig. 4B and C; Table 1).

Air breaths of *P. annectens* began with the synchronous depression of the lower jaw and ceratohyal, shortly followed by the synchronous depression of the clavicle and cranial rib (Fig. 4B and C). The lower jaw reached peak depression first ($43.44 \pm 1.83\%$ breath duration), followed by the ceratohyal ($50.75 \pm 1.32\%$ breath duration), the clavicle ($50.77 \pm 1.70\%$ breath duration), and lastly, the cranial rib ($51.97 \pm 1.96\%$ breath duration). Rotation of the clavicles, as well as the cranial ribs and lower jaw, tended to plateau between retraction and protraction. Clavicle retraction sometimes peaked at the beginning of the plateau (as was seen more often in Pa04), and sometimes peaked at the end (as was seen more often in Pa01), leading to variability between Pa01 and Pa04 in whether the clavicle peaked before or after the ceratohyal (Table 1). Which bones rotated the most and least were consistent between breaths and individuals. The ceratohyal depressed the most ($-42.2 \pm 3.5^\circ$), the clavicle retracted the second most ($-25.0 \pm 1.4^\circ$), and the lower jaw ($-17.6 \pm 0.7^\circ$, mean ± s.e.m.) and cranial rib ($-15.0 \pm 0.7^\circ$) rotated the least (Table 1).

Skeletal kinematics during suction feeding

The suction strikes of Pa04 began with the synchronous depression of the lower jaw and ceratohyal, shortly followed by the synchronous depression of the clavicle and cranial rib (Fig. 4D). The lower jaw reached peak depression ($-12.5 \pm 2.8^\circ$) 210 ± 50 ms after the start of the strike. The ceratohyal reached its peak depression ($-37.2 \pm 6.3^\circ$) next, 358 ± 72 ms after the start of the strike. The clavicle followed, depressing to $-19.8 \pm 3.53^\circ$, peaking 415 ± 88 ms after the start of the strike. Lastly, the cranial rib retracted to $-7.3 \pm 1.3^\circ$, peaking 458 ± 103 ms after the start of the strike (Fig. 4D; Table 2). The single suction strike recorded from Pa01 had the same relative amounts of rotation of each bone as in the strikes recorded from Pa04, but differed somewhat in the sequence of peak bone rotations, as the cranial rib reached peak retraction last in this strike (Fig. 4E; Table 2).

Length changes of the costo-clavicular portion of the hypaxial muscles (CCH) during air breathing and suction feeding

The CCH shortened substantially during both air breathing ($16.4 \pm 0.9\%$ L_i) and suction feeding ($14.6 \pm 2.6\%$ L_i). During both behaviors, it began shortening at nearly the same time as the start of depression of the clavicle and cranial rib, and it reached peak shortening at approximately the same time as the ceratohyals (Fig. 4; Tables 1 and 2).

During air breathing, there were two distinct bouts of CCH shortening (Fig. 4B and C). During buccal expansion, the CCH shortened, reaching peak strain at $51.22 \pm 1.57\%$ breath duration. During buccal compression,

Table 2 Mean magnitude and timing of bone rotation and muscle shortening during suction feeding.

Variable		Pa01 (n = 1)	Pa04 (n = 3)	Combined
Strike duration (ms)		1073	1211 ± 66	1177 ± 58
Lower jaw	Peak depression* (°)	−7.8	−14.0 ± 3.3	−12.5 ± 2.8
	Time to peak depression (ms)	313	176 ± 50	210 ± 50
Ceratohyal (left)	Peak depression* (°)	−21.7	−42.3 ± 5.2	−37.2 ± 6.3
	Time to peak depression (ms)	540	298 ± 56	358 ± 72
Clavicle (left)	Peak retraction* (°)	−11.8	−22.4 ± 3.3	−19.8 ± 3.5
	Time to peak retraction (ms)	627	344 ± 73	415 ± 88
Cranial rib (left)	Peak retraction* (°)	−5.9	−7.7 ± 1.8	−7.3 ± 1.3
	Time to peak retraction (ms)	687	382 ± 98	458 ± 103
Costoclavicular portion of hypaxial muscles (CCH, left)	Peak strain** (% L_i)	9.0	16.4 ± 2.6	14.6 ± 2.6
	Time to peak shortening (ms)	527	318 ± 54	370 ± 65

*Negative values indicate depression or retraction.

**Positive values indicate muscle shortening. Mean ± s.e.m. are shown for each variable. Strike duration measured from start of lower jaw depression to end of clavicle protraction. Magnitude and timing of peaks were measured relative to start of behavior (start of lower jaw depression).

sion, as the clavicles began to protract, the cranial rib seemed to remain retracted (in the plateau portion of its curves, as described above), while the CCH lengthened slightly. Then, the CCH began shortening again, returning to approximately the same length as in the first bout of shortening (Fig. 4B and C). Qualitatively, during this second bout of CCH shortening, the elevation of the clavicles slowed down, and the protraction of the cranial rib sped up. This shortening also occurred at the same time as the start of lung inflation. After shortening briefly, the CCH lengthened to its initial length.

Discussion

Air breathing and suction feeding share similar skeletal kinematics and muscle shortening patterns. In both buccal pumping behaviors, the clavicles and cranial ribs consistently contributed to buccal expansion by retracting considerably, as well as serving as anchors for their associated muscles. The CCH shortened during buccal expansion, likely assisting retraction of the clavicle. Although suction feeding was a much faster behavior and had a faster expansion phase than compression phase compared to air breathing, both behaviors shared the same sequence of bone rotation during expansion and during compression, and the ranked magnitudes of peak bone rotation were also the same. Overall, we found that air breathing and suction feeding used the same mechanisms for buccal pumping, and therefore, despite differences in duration of the behaviors, air breathing in *P. annectens* does not require specialized anatomy or kinematics.

Skeletal kinematics of air breathing and suction feeding

While the small number of suction feeding strikes in our dataset limits the quantitative analyses we can perform, we are able to compare air breathing and suction feeding qualitatively in terms of the mechanisms and kinematics involved. Comparing the behaviors at this more fundamental level is perhaps the best way to address our question of whether air breathing requires specialized biomechanics.

Air breathing and suction feeding were characterized by the same sequence of bone motion, ranked magnitudes of bone rotation, and the roles that the bones played. In both behaviors, the clavicle and cranial rib rotated consistently and substantially as a continuation of the anterior-to-posterior waves of expansion and compression: the lower jaw, ceratohyals, clavicles, and cranial rib were depressed/retracted, in that order, and then those bones elevated/protracted, in that order as well (Fig. 4; Tables 1 and 2). The ceratohyals rotated the most, and the clavicles rotated the second most, acting to greatly expand the buccal cavity. The cranial rib rotated the least, contributing somewhat to buccal expansion while also serving as an anchor for the CCH and other hypaxial muscle fibers. And the lower jaw rotated slightly more than the cranial rib, acting as a valve to control the flow of fluid.

Air breathing and suction feeding differed in the duration of the behavior and the relative durations of expansion and compression. Although feeding on non-evasive prey is quite slow in lungfish (Bemis and Lauder 1986; Gartner et al. 2022), suction feeding was more than three times faster than air breathing, and in suction feeding, buccal expansion occurred much more quickly than buccal compression (Fig. 4; Tables 1 and

2). In contrast, during air breathing, buccal expansion took approximately as long as buccal compression. It is possible that the differences in temporal duration between the two behaviors are due to the different fluid mechanics of the two situations. In suction feeding, the prey must be rapidly accelerated within a bolus of water and prevented from exiting the buccal cavity, requiring a rapid expansion phase and a variable compression phase. Flow is largely unidirectional. On the other hand, air breathing simply requires buccal expansion, allowing air to be expired and fresh air to be drawn in, and buccal compression, with a sealed oral valve, to force the air to move caudally into the lungs.

The larger suction feeding dataset in [Gartner et al. \(2022\)](#), which was collected from the same *P. annectens* individuals as our study, is consistent with the kinematic patterns we report here. The lower jaw rotated less ($-11.6 \pm 0.2^\circ$; mean \pm s.e.m. for $n = 34$, combined from both Pa01 and Pa04) than the ceratohyal ($-21.88 \pm 0.4^\circ$) and reached peak depression (264 ± 5 ms) well before the ceratohyal (364 ± 5 ms) ([Gartner et al. 2022](#)). The air breaths presented in our study reached peak ceratohyal depression more than five times slower than both the suction feeding strikes presented in our study and the suction feeding strikes presented in [Gartner et al. \(2022\)](#), which had a mean time to peak ceratohyal depression of 367 ± 30 ms. This larger dataset did not include cranial rib and clavicle motions, so we cannot compare those motions between the datasets.

During air breathing, some air was expelled through the oral valve in the beginning of buccal compression, rather than being forced into the lungs. This was a consequence of the ceratohyals elevating at approximately the same time that the lower jaw began elevating, but before the lips were sealed. This pattern was less apparent during suction feeding, where the timing of lower jaw and ceratohyal elevation was less tightly coupled. It is possible that because the ceratohyal depressed more during air breathing, the mandibulohyoid ligament was pulled taut and acted as a physical constraint, pulling the ceratohyal up when the lower jaw elevated.

Role of the oral valve in air breathing and suction feeding

[Bishop and Foxon \(1968\)](#) hypothesized that the tongue plays an important role in sealing the mouth anteriorly during lung inflation (i.e., inspiration) in *Lepidosiren paradoxa*, arguing that although the lips are closed, they are not the main mechanism for sealing the mouth. However, we found that during much of lung inflation, the tongue was not contributing to sealing the mouth. During approximately the first half of lung inflation,

the tongue did not touch the cranium, and only mid-way through lung inflation were the ceratohyals elevated far enough for the tongue to press against the cranium. [McMahon \(1969\)](#) reported that buccal pressure increased steadily until intrapulmonary pressure began to plateau (indicating that the lungs were nearly full), at which point the buccal pressure increased rapidly ([McMahon 1969](#)). This suggests that the jaws and lips were able to seal the buccal cavity enough for there to be a buildup of buccal pressure.

We hypothesize that the primary role of the tongue is to maximize the transfer of air from the buccal cavity to the lungs. During the first part of lung inflation, while the tongue is depressed, it is possible that some air leaked out through the lips, but this seems unlikely for three reasons: (1) air leakage was not visible in our X-ray videos; (2) buccal pressure is lower earlier in lung inflation; and (3) the lips are being pressed together by strong jaw closing muscles, capable of crushing shells ([Shinkafi and Maradun 2009](#)). In the later part of lung inflation, the tongue pressed against the roof of the mouth, which likely both assisted the lips in sealing the oral valve and maximized the amount of air that is forced into the lungs during inflation. This second role is perhaps more functionally important, and the first role (sealing) may simply be a consequence of performing the second role.

The motions of the tongue during suction feeding were similar to those during air breathing. During both behaviors, the tongue remained depressed for the first part of buccal compression and then pressed against the roof of the mouth once the ceratohyals were elevated. Unlike during air breathing, completely sealing the oral valve (using the lips or the tongue) is not necessary during suction feeding, nor is maximizing compression of the buccal cavity. Still, as in air breathing, it is possible that any role that the tongue plays in sealing the oral valve during suction feeding is simply a consequence of the tongue being elevated during buccal compression.

CCH muscle shortening

During both air breathing and suction feeding, the CCH shortened during expansion of buccal cavity ([Fig. 4](#)). We hypothesize that this increased the velocity of retraction of the clavicle, while the retractor costalis acted to resist the anterior pull of the CCH, as well as retract the cranial rib. Because the CCH began shortening at the same time that the clavicle and cranial rib began retracting, we cannot say, based on our data, whether the clavicle and cranial rib would have rotated faster or slower in the absence of CCH shortening. Further research is needed to test this hypothesis.

Potential accessory mechanism of ventilation during estivation

We hypothesize that cranial rib motion may assist slightly in compressing and expanding the lungs. Anterodorsally, the lung walls cover the posterior surface of the retractor costalis, as well as the ventral surfaces of the pleural ribs and vertebrae. As the cranial rib moves, the region of lung wall that covers the retractor costalis moves as well, and so cranial rib motion inherently affects lung volume, though to a limited extent.

This hypothesis is supported by our data during air breathing. During buccal expansion, which is simultaneous with lung deflation (i.e., expiration), the cranial ribs were actively retracted; therefore, they pushed on the anterodorsal regions of the lungs. We hypothesize that this rib retraction may make a small contribution to expiratory volume but that hydrostatic pressure, and possibly the smooth muscle in the lung wall, is the primary mechanism of lung deflation. At the start of lung inflation, the CCH shortened briefly. Because clavicle and cranial rib protraction had begun before the CCH shortening started, we were able to observe qualitatively that the velocity of clavicle protraction (and of ceratohyal elevation) decreased, while the velocity of cranial rib protraction increased (Fig. 4B and C). Therefore, we hypothesize that shortening of the CCH at the start of lung inflation functions to assist protraction of the cranial rib and may help initiate lung inflation. However, the shortening of the CCH was brief and the effect of cranial rib motion on lung volume appeared to be small, so buccal force pumping remains the primary mechanism of lung inflation.

Although we conclude that movement of the cranial rib likely produces just a small amount of volume change, it is intriguing to think how it might assist during estivation. *Protopterus annectens* estivate during the dry season in shallow subterranean burrows that have a short tunnel that connects the fish's mouth to the atmosphere (Greenwood 1986). Lungfish secrete mucus that hardens into a cocoon (Greenwood 1986). Without access to water, the fish relies entirely on its lungs to obtain oxygen, taking small breaths to meet its lowered metabolic demand (Smith 1930; Lomholt et al. 1975; Delaney and Fishman 1977). The kinematics of air breathing must be different during estivation. Hydrostatic pressure cannot cause lung deflation, and the cocoon restricts buccal expansion (Smith 1930; Lomholt et al. 1975). During these conditions, the motions of the cranial rib may play a more important role in the small tidal volume breaths taken during estivation. Studies on the mechanisms of air breathing in estivating lungfish have conflicting results, creating uncertainty about whether lungfish are able to seal their mouths, which is

necessary for buccal pumping, or whether they are using aspiration (Lomholt et al. 1975; Delaney and Fishman 1977). However, in either case, cranial rib retraction could contribute to lung deflation, and cranial rib protraction could contribute to lung inflation, either by assisting buccal pumping or as a mechanism for aspiration breathing.

Origin of air breathing

The ancestors of the first air-breathing fish used buccal pumping for gill ventilation and feeding (Hughes 1965; Wainwright et al. 2015). Later, air breathing evolved as an additional buccal pumping behavior, but one that moved air through the head, rather than water (Brainerd 1994). As they are both buccal pumping behaviors, air breathing and suction feeding share some similarities in their functional requirements. Suction feeding requires an anterior-to-posterior wave of expansion to accelerate water into the buccal cavity, an anterior-to-posterior wave of compression to maintain the posterior unidirectional flow, and rapid and large buccal expansion to generate effective subambient buccal pressure (Bishop et al. 2008). On the other hand, air breathing simply requires buccal expansion to draw air in and buccal compression, with a sealed oral valve, to force the air to move into the lungs. The shared need for buccal expansion and compression is the reason that both behaviors are successfully accomplished using buccal pumping. However, different fluid dynamics and objectives of the behaviors make it unclear whether these behaviors are also similar beyond simply using buccal expansion and compression. Our findings demonstrate that air breathing and suction feeding not only are performed using the same basic mechanism, a buccal force pump, but also use similar kinematic and muscle shortening patterns. The cranial morphology that enables suction feeding is well suited to perform air breathing and accommodate both the physical differences between air and water and the differences in the objectives of the behaviors.

While we do not consider its effects in this study, surface tension is a physical property that varies between air and water and can be a substantial barrier to accessing the air for very small animals such as tadpoles (Phillips et al. 2020; Schwenk and Phillips 2020). At this time there is no reason to think that air breathing evolved in small-bodied species, but surface tension should be considered as a potential barrier to air breathing in small species and the early life history stages of larger species.

Our data do not address the question of whether air breathing evolved from suction feeding, gill ventilation, or another behavior. As many prior authors

have discussed, the buccal pumps used for air ventilation may have evolved from buccal pumps used for gill ventilation, aquatic coughing, and/or feeding (McMahon 1969; Gans 1970; Liem 1985; Smatresk 1990; Brainerd 1994; Brainerd and Ferry-Graham 2006; Brainerd 2015). While our data show that air breathing and suction feeding share similar kinematic and muscle shortening patterns, it is likely that gill ventilation also shares these patterns, and so these similarities are not evidence that air breathing necessarily evolved by modification of suction feeding. Rather, our data demonstrate that the skeletal kinematics required for aquatic and aerial buccal pumps need not be markedly different.

Perhaps it is appropriate to consider air breathing as easier to evolve than we might expect at first glance. In contrast to the origin of a behavior such as terrestrial locomotion, which required substantial changes to morphology and kinematics, it seems that the origin of air breathing did not. The kinematics of air breathing are fundamentally similar to those of suction feeding (and likely gill ventilation as well), suggesting that the origin of air breathing did not require substantial changes to cranial kinematics. In this way, air breathing may be an exception to our expectations about what it takes to adapt to interacting with a new physical medium.

Acknowledgments

We are grateful to Callum Ross for research administrative support, to David Baier for the XROMM Maya Tools, to the Harvard Museum of Comparative Zoology for providing specimens, to the University of Chicago Animal Resource Center staff, to Neil Shubin and members of his laboratory for lending supplies for PMA staining, to J.D. Laurence-Chasen for assistance optimizing X-ray video quality, and to Shuah Yu for tracking the videos.

Funding

This work was supported by the National Science Foundation [grant numbers IOS-1655756 to E.L.B., DGE-1644760 to E.B.K., DEB-1541547 to M.W.W., DBI-1338066 to Callum F. Ross, OAC-1626552 to Hakizumwami B. Runesha]; the Bushnell Research and Education Fund [to E.B.K.]; and the University of Chicago [to S.M.G.]. This is University of Chicago XROMM Facility Publication #13.

Supplementary data

Supplementary data available at *ICB* online.

Conflict of interest

We declare no competing or financial interests.

Data availability

X-ray video and CT data and their essential metadata for this publication have been deposited in the University of Chicago XMA Portal (<https://xromm.rcc.uchicago.edu>) in the study “Lungfish Breathing,” with the permanent identifier “portal_base8,” and in the study “Lungfish Feeding,” with the permanent identifier “portal_base4,” and will be publicly available under CCBY 4.0 upon publication.

References

- Aiello BR, King HM, Hale ME. 2014. Functional subdivision of fin protractor and retractor muscles underlies pelvic fin walking in the African lungfish *Protopterus annectens*. *J Exp Biol* 217:3474–82.
- Babiker MM. 1979. Respiratory behaviour, oxygen consumption and relative dependence on aerial respiration in the African lungfish (*Protopterus annectens*, Owen) and an air-breathing teleost (*Clarias lazera*, C.). *Hydrobiologia* 65: 177–87.
- Bemis WE, Lauder GV. 1986. Morphology and function of the feeding apparatus of the lungfish, *Lepidosiren paradoxa* (Dipnoi). *J Morphol* 187:81–108.
- Betancur-R R, Wiley EO, Arratia G, Acero A, Bailly N, Miya M, Lecointre G, Ortí G. 2017. Phylogenetic classification of bony fishes. *BMC Evol Biol* 17:1–40.
- Bishop IR, Foxon GEH. 1968. The mechanism of breathing in the South American lungfish, *Lepidosiren paradoxa*; radiological study. *J Zool* 154:263–71.
- Bishop KL, Wainwright PC, Holzman R. 2008. Anterior-to-posterior wave of buccal expansion in suction feeding fishes is critical for optimizing fluid flow velocity profile. *J R Soc Interface* 5:1309–16.
- Brainerd EL, Baier DB, Gatesy SM, Hedrick TL, Metzger KA, Gilbert SL, Crisco JJ. 2010. X-ray reconstruction of moving morphology (XROMM): precision, accuracy and applications in comparative biomechanics research. *J Exp Zool Part A Ecol Genet Physiol* 313A:262–79.
- Brainerd EL, Blob RW, Hedrick TL, Creamer AT, Müller UK. 2017. Data management rubric for video data in organismal biology. *Integr Comp Biol* 57:33–47.
- Brainerd EL, Ferry-Graham LA. 2006. Mechanics of respiratory pumps. *Fish Physiol* 23:1–28.
- Brainerd EL, Moritz S, Ritter DA. 2016. XROMM analysis of rib kinematics during lung ventilation in the green iguana, *Iguana iguana*. *J Exp Biol* 219:404–11.
- Brainerd EL. 1994. The evolution of lung–gill bimodal breathing and the homology of vertebrate respiratory pumps. *Am Zool* 34:289–99.
- Brainerd EL. 2015. Major transformations in vertebrate breathing mechanisms. In: Dial KP, Shubin N, Brainerd EL, editors. *Great transformations in vertebrate evolution*. Chicago, IL: University of Chicago Press. p. 47–62.

- Camp AL, Brainerd EL. 2014. Role of axial muscles in powering mouth expansion during suction feeding in largemouth bass (*Micropterus salmoides*). *J Exp Biol* 217:1333–45.
- Capano JG, Moritz S, Cieri RL, Reveret L, Brainerd EL. 2019. Rib motions don't completely hinge on joint design: costal joint anatomy and ventilatory kinematics in a teiid lizard, *Salvator merianae*. *Integr Org Biol* 1–18. doi:10.1093/iob/oby004.
- Clack JA. 2009. The fish-tetrapod transition: new fossils and interpretations. *Evol Educ Outreach* 2:213–23.
- Coates MI, Ruta M, Friedman M. 2008. Ever since Owen: changing perspectives on the early evolution of tetrapods. *Annu Rev Ecol Evol Syst* 39:571–92.
- Damsgaard C, Baliga VB, Bates E, Burggren WW, McKenzie DJ, Taylor E, Wright PA. 2020. Evolutionary and cardio-respiratory physiology of air-breathing and amphibious fishes. *Acta Physiol* 228:e13406.
- Delaney RG, Fishman AP. 1977. Analysis of lung ventilation in the aestivating lungfish *Protopterus aethiopicus*. *Am J Physiol Regul Integr Comp Physiol* 2:R181–7.
- Farmer CG. 1999. Evolution of the vertebrate cardio-pulmonary system. *Annu Rev Physiol* 61:573–92.
- Gans C. 1970. Strategy and sequence in the evolution of the external gas exchangers of ectothermal vertebrates. *Forma Funct* 3:61–104.
- Gartner SM, Whitlow KR, Laurence-Chasen JD, Granatosky MC, Ross CF, Westneat MW. 2022. Suction feeding of West African lungfish (*Protopterus annectens*): XROMM analysis of jaw mechanics, cranial kinesis, and hyoid mobility. *bioRxiv* <https://doi.org/10.1101/2022.05.30.493759>.
- Graham JB. 1997. Air-breathing fishes: evolution, diversity, and adaptation. San Diego, CA: Academic Press.
- Granatosky MC, Laurence-Chasen JD, Gartner SM, Whitlow KR, Westneat MW, Nyakatura JA. 2020. An XROMM and kinetic analysis of underwater walking in the West African lungfish (*Protopterus annectens*) with implications for the role of quadrupedal gaits during the fin-to-limb transition. *Integr Comp Biol* 60:E88.
- Greenwood PH. 1986. The natural history of African lungfishes. *J Morphol* 190:163–79.
- Horner AM, Jayne BC. 2014. Lungfish axial muscle function and the vertebrate water to land transition. *PLoS One* 9:e96516.
- Hughes GM. 1965. Comparative physiology of vertebrate respiration. Vol. 2. Cambridge, MA: Harvard University Press.
- King HM, Hale ME. 2014. Musculoskeletal morphology of the pelvis and pelvic fins in the lungfish *Protopterus annectens*. *J Morphol* 275:431–41.
- Knörlein BJ, Baier DB, Gatesy SM, Laurence-Chasen JD, Brainerd EL. 2016. Validation of XMALab software for marker-based XROMM. *J Exp Biol* 219:3701–11.
- Liem KF. 1985. Ventilation. Hildebrand M, Bramble DM, Liem KF, Wake DB, editors. *Functional vertebrate morphology*. Cambridge (MA): Harvard University Press. p. 186–209.
- Lomholt JP, Johansen K, Maloij GMO. 1975. Is the aestivating lungfish the first vertebrate with suctional breathing? *Nature* 257:787–8.
- Long JA, Gordon MS. 2004. The greatest step in vertebrate history: a paleobiological review of the fish-tetrapod transition. *Physiol Biochem Zool* 77:700–19.
- MacIver MA, Finlay BL. 2021. The neuroecology of the water-to-land transition and the evolution of the vertebrate brain. *Philos Trans R Soc Lond B Biol Sci* 377:20200523.
- McMahon BR. 1969. A functional analysis of the aquatic and aerial respiratory movements of an African lungfish, *Protopterus aethiopicus*, with reference to the evolution of the lung-ventilation mechanism in vertebrates. *J Exp Biol* 51: 407–30.
- Olsen AM, Hernández LP, Camp AL, Brainerd EL. 2019. Channel catfish use higher coordination to capture prey than to swallow. *Proc R Soc B* 286. doi:10.1098/rspb.2019.0507.
- Phillips JR, Hewes AE, Schwenk K. 2020. The mechanics of air breathing in gray tree frog tadpoles, *Hyla versicolor* (Anura: Hylidae). *J Exp Biol* 223. doi:10.1242/jeb.219311.
- Rosen DE, Forey PL, Gardiner BG, Patterson C. 1981. Lungfishes, tetrapods, paleontology, and plesiomorphy. *Bull Am Mus Nat Hist* 167:159–276.
- Sayer MDJ. 2005. Adaptations of amphibious fish for surviving life out of water. *Fish Fish* 6:186–211.
- Schwenk K, Phillips JR. 2020. Circumventing surface tension: tadpoles suck bubbles to breathe air. *Proc R Soc B* 287. doi:10.1098/rspb.2019.2704.
- Shinkafi BA, Maradun HF. 2009. Food and feeding habits of *Protopterus annectens* (Owen) in River Rima, Sokoto, Nigeria. *Fish Soc Niger* 56–60.
- Shubin NH, Daeschler EB, Jenkins FA. 2006. The pectoral fin of Tiktaalik roseae and the origin of the tetrapod limb. *Nature* 440:764–71.
- Smatresk NJ. 1990. Chemoreceptor modulation of endogenous respiratory rhythms in vertebrates. *Am J Physiol Regul Integr Comp Physiol* 259:R887–97.
- Smith HW. 1930. Metabolism of the lungfish, *Protopterus aethiopicus*. *J Biol Chem* 88:97–130.
- Takezaki N, Figueroa F, Zaleska-Rutczynska Z, Takahata N, Klein J. 2004. The phylogenetic relationship of tetrapod, coelacanth, and lungfish revealed by the sequences of forty-four nuclear genes. *Mol Biol Evol* 21:1512–24.
- Wainwright PC, McGee MD, Longo SJ, Patricia Hernandez L. 2015. Origins, innovations, and diversification of suction feeding in vertebrates. *Integr Comp Biol* 55:134–45.